Bottomonium Suppression in the QGP

Michael Strickland
Kent State University

Institute for Nuclear Theory
Heavy Flavor and Electromagnetic Probes in Heavy Ion Collisions

KENT STATE UNIVERSITY

JET Collaboration

HIC for FAIR
Helmholtz International Center

Outline

- Why bottomonium?
- Non-equilibrium plasma dynamics
  (→ plasma momentum-space anisotropy)
- Incorporating anisotropy in the heavy quark potential
- Putting the pieces together
- Results
- What are we doing now?
- Conclusions

Why Bottomonium?

- Bottom quarks ($m_b \approx 4.2$ GeV) are more massive than charm quarks ($m_c \approx 1.3$ GeV) and, as a result, the heavy quark effective theories underpinning phenomenological applications are on somewhat surer footing.
- Due to their higher mass, the effects of initial state (IS) nuclear suppression are expected to be smaller than for the charmonium states. At forward/backward rapidities, however, IS effects on bottomonium could still be very important.
- The masses of bottomonium states ($m_\Upsilon \approx 10$ GeV) are much higher than the temperatures (T < 1 GeV) generated in HICs → bottomonia production will be dominated by initial hard scatterings.
- Since bottom quarks and anti-quarks are relatively rare, the probability for regeneration of bottomonium states through statistical recombination is much smaller than for charm quarks. (Still can be "correlational pairing" though…)

Vacuum Quarkonia Spectra

Bottomonia

State	Name	Exp. [92]	Model	Rel. Err.
1^1S_0	$\eta_b(1S)$	9.398 GeV	9.398 GeV	0.001%
1^3S_1	$\Upsilon(1S)$	9.461 GeV	9.461 GeV	0.004%
1^3P_0	$\chi_{b0}(1P)$	9.859 GeV	9.869 GeV	0.21%
1^3P_1	$\chi_{b1}(1P)$	9.893 GeV		
1^3P_2	$\chi_{b2}(1P)$	9.912 GeV		
1^1P_1	$h_b(1P)$	9.899 GeV		
2^1S_0	$\eta_b(2S)$	9.999 GeV	9.977 GeV	0.22%
2^3S_1	$\Upsilon(2S)$	10.002 GeV	9.999 GeV	0.03%
2^3P_0	$\chi_{b0}(2P)$	10.232 GeV	10.246 GeV	0.05%
2^3P_1	$\chi_{b1}(2P)$	10.255 GeV		
2^3P_2	$\chi_{b2}(2P)$	10.269 GeV		
2^1P_1	$h_b(2P)$	-		
3^1S_0	$\eta_b(3S)$	-	10.344 GeV	-
3^3S_1	$\Upsilon(3S)$	10.355 GeV	10.358 GeV	0.03%

Cornell potential + spin-spin interaction fixed to lattice

J. Alford and MS, 1309.3003

Charmonia

State	Name	Exp. [92]	Model	Rel. Error
1^1S_0	$\eta_c(1S)$	2.984 GeV	3.048 GeV	2.2%
1^3S_1	$J/\psi(1S)$	3.097 GeV	3.100 GeV	0.11%
2^1S_0	$\eta_c(2S)$	3.639 GeV	3.721 GeV	2.3%
2^3S_1	$J/\psi(2S)$	3.686 GeV	3.748 GeV	1.7%

- With a simple pNRQCD potential model one can describe the known bottomonia state masses with a maximum error of 0.22%
- The situation with charmonia is a bit worse and one has to add relativistic corrections with additional parameters.

LHC Heavy Ion Collision Timescales

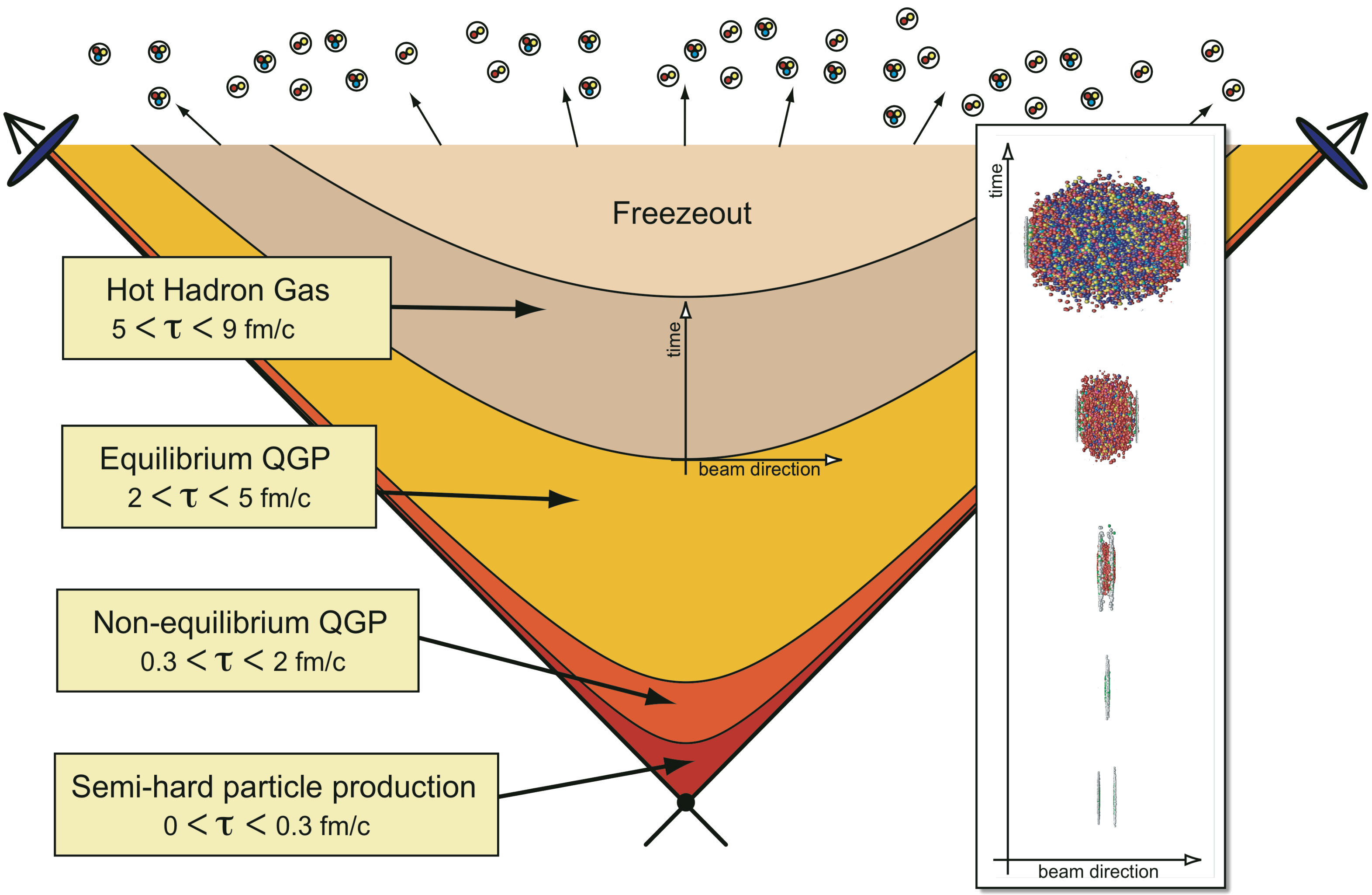

QGP momentum anisotropy cartoon

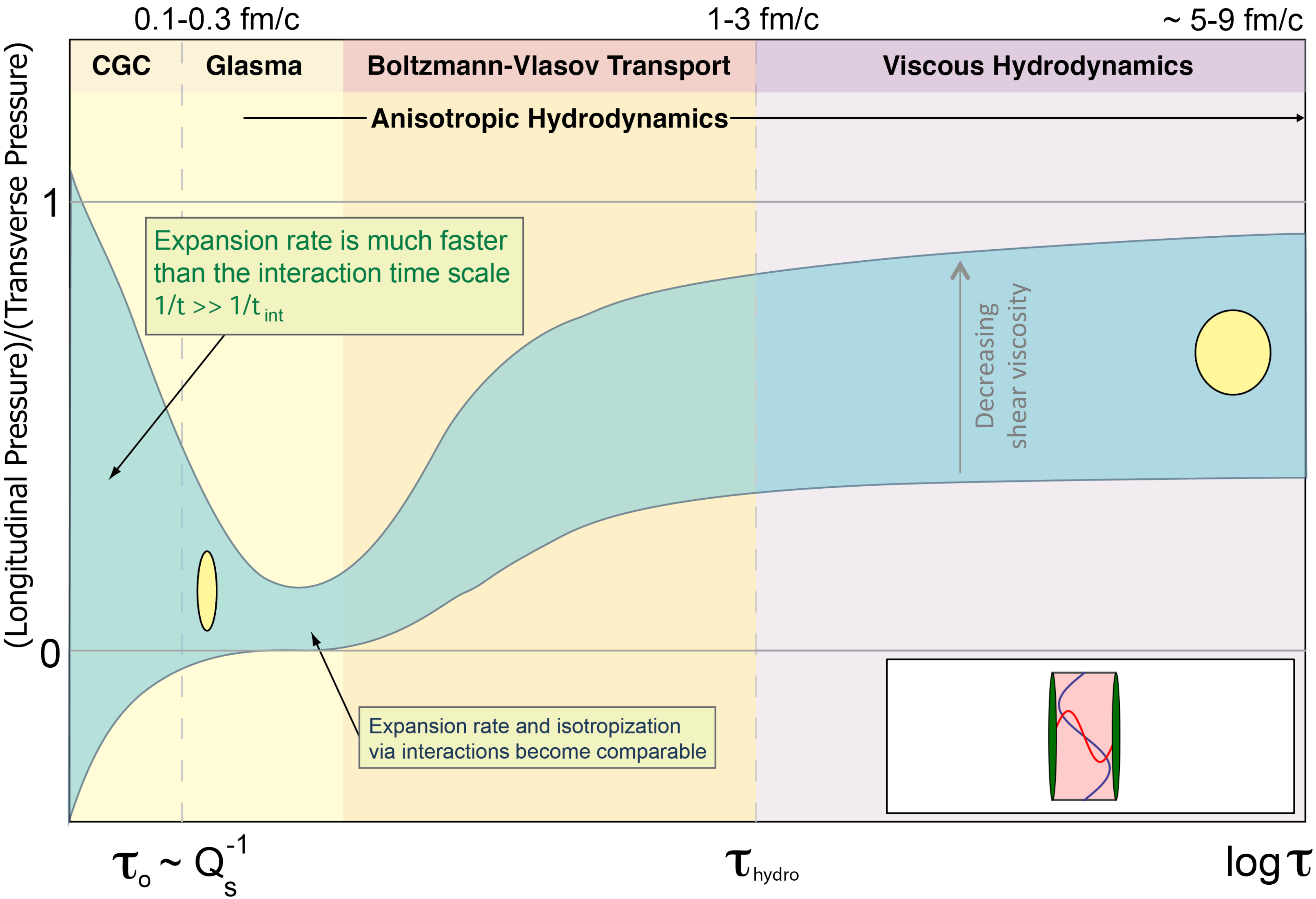

Estimating Early-time Pressure Anisotropy

- CGC @ leading order predicts negative → approximately zero longitudinal pressure
- QGP scattering + plasma instabilities work to drive the system towards isotropy on the fm/c timescale, but don't seem to fully restore it
- Viscous hydrodynamics predicts early-time anisotropies ≤ 0.35 → 0.5 (see next slide)
- AdS-CFT dynamical calculations in the strong coupling limit predict anisotropies of ≤ 0.3 (discussion in three slides from now)

Estimating Anisotropy – Viscous hydro

- To get a feeling for the magnitude of pressure anisotropies to expect, let's consider the Navier-Stokes limit

$$\boxed{\left(\frac{\mathcal{P}_L}{\mathcal{P}_T}\right)_{\rm NS} = \frac{P_{\rm eq} + \pi^{zz}_{\rm NS}}{P_{\rm eq} + \pi^{xx}_{\rm NS}} = \frac{3\tau T - 16\bar\eta}{3\tau T + 8\bar\eta}}$$

$$\boxed{\bar\eta = \frac{\eta}{\mathcal{S}}}$$

$$\boxed{\pi^{zz}_{\rm NS} = -2\pi^{xx}_{\rm NS} = -2\pi^{yy}_{\rm NS} = -4\eta/3\tau}$$

- P_L/P_T decreases with increasing η/S
- P_L/P_T decreases with decreasing T
- Assume $\eta/S = 1/4\pi$ in order to get an upper bound on the anisotropy
- Using RHIC initial conditions (T_0 = 400 MeV @ τ_0 = 0.5 fm/c) we obtain $P_L/P_T \leq 0.5$
- Using LHC initial conditions (T_0 = 600 MeV @ τ_0 = 0.25 fm/c) we obtain $P_L/P_T \leq 0.35$
- Negative P_L at large η/S or low temperatures!?

Estimating Anisotropy – Viscous hydro

- Navier-Stokes solution is "attractor" for the 2nd order solution
- τ_π sets timescale to approach Navier-Stokes evolution
- $\tau_\pi \sim 5\eta/(TS) \sim 0.1$ fm/c at LHC temperatures
- Assume isotropic LHC initial conditions T_0= 600 MeV @ τ_0 = 0.25 fm/c and solve for the 0+1d viscous hydro dynamics

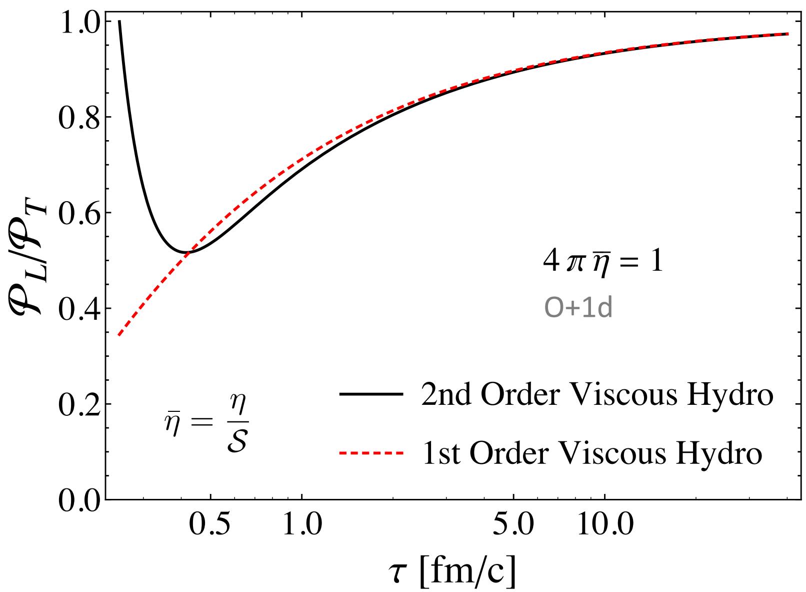

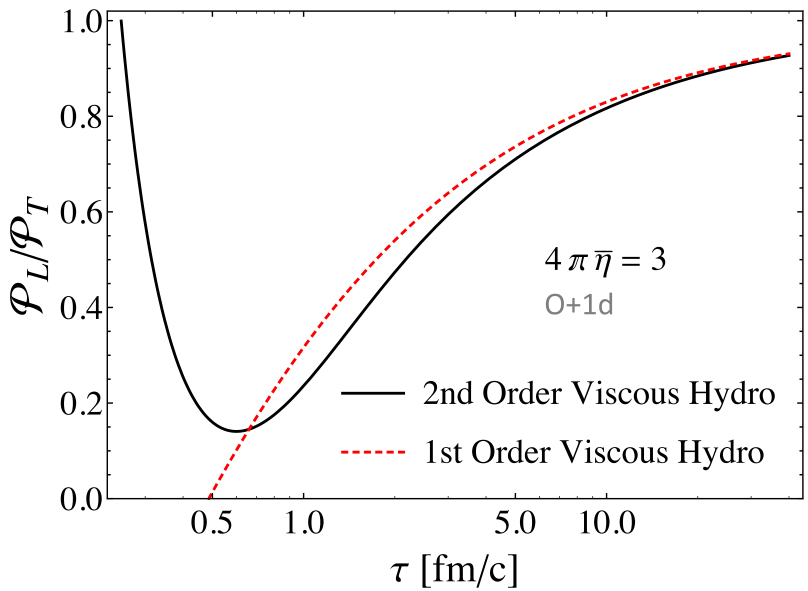

Estimating Anisotropy – AdS/CFT

- In 0+1d case there are now numerical solutions of Einstein's equations to compare with.
  [Heller, Janik, and Witaszczyk, 1103.3452]

- They studied a wide variety of initial conditions and found a kind of universal lower bound for the thermalization time.

$$\langle T_{\tau\tau}\rangle \equiv \varepsilon(\tau) \equiv N_c^2 \cdot \frac{3}{8}\pi^2 \cdot T_{eff}^4 \cdot$$

$$w = T_{eff} \cdot \tau$$

$$\frac{\tau}{w}\frac{d}{d\tau}w = \frac{F_{hydro}(w)}{w},$$

F_{hydro} known up to 3rd order hydro analytically

RHIC 200 GeV/nucleon:
T_0 = 350 MeV, τ_0 > 0.35 fm/c

LHC 2.76 TeV/nucleon:
T_0 = 600 MeV, τ_0 > 0.2 fm/c

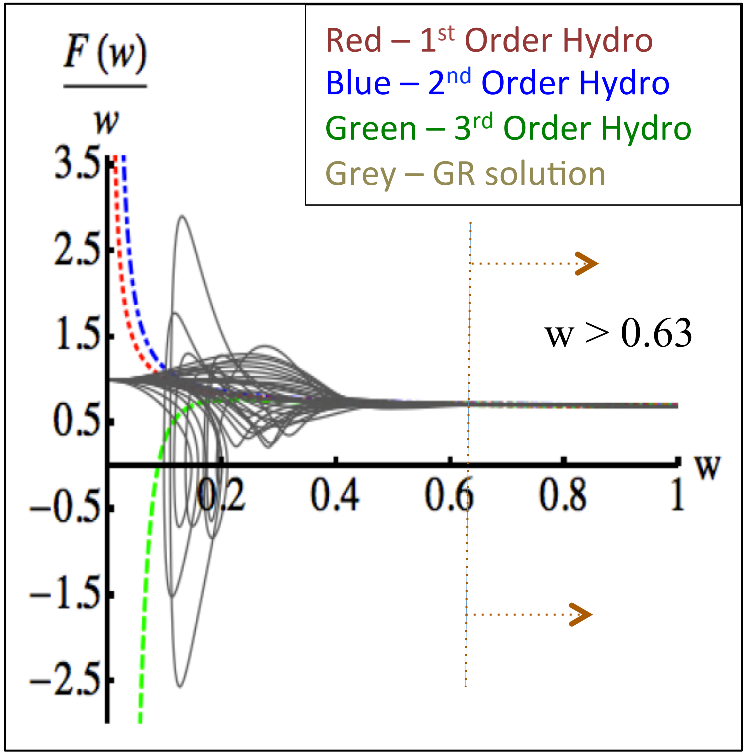

N=4 SUSY using AdS/CFT

However, at that time the system is not isotropic and remains anisotropic for the entirety of the evolution

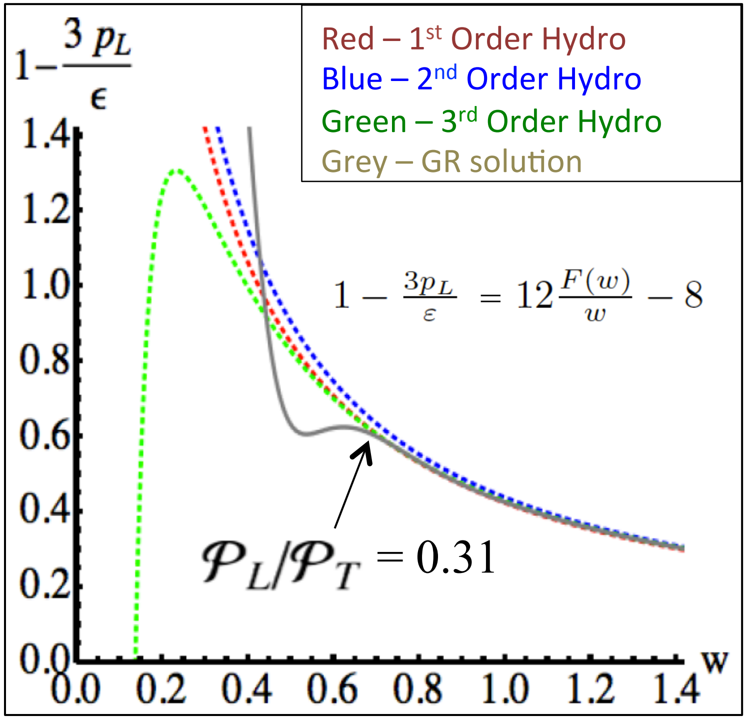

Other AdS/CFT numerical studies which include transverse expansion reach a similar conclusion
[van der Schee et al. 1307.2539]

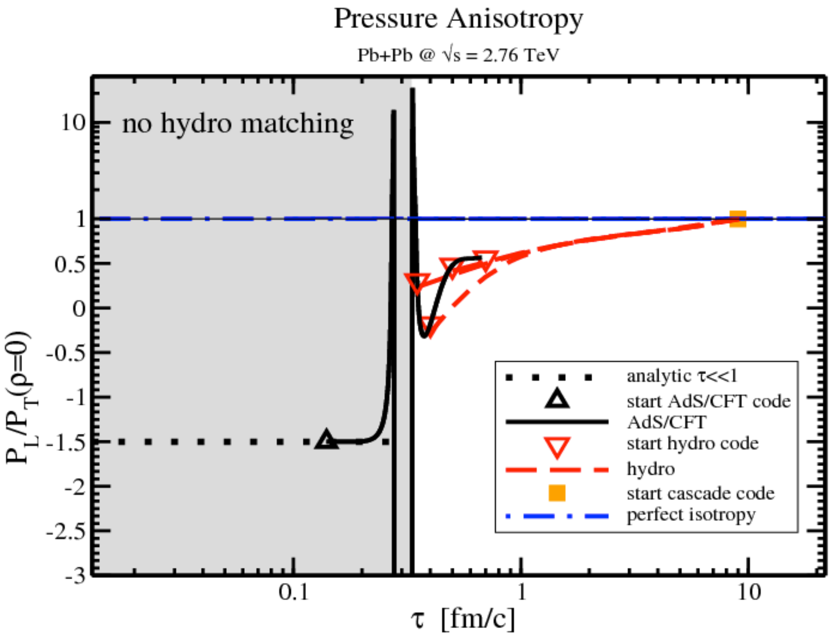

See also J. Casalderrey-Solana et al. arXiv: 1305.4919

Temperature dependence of η/S

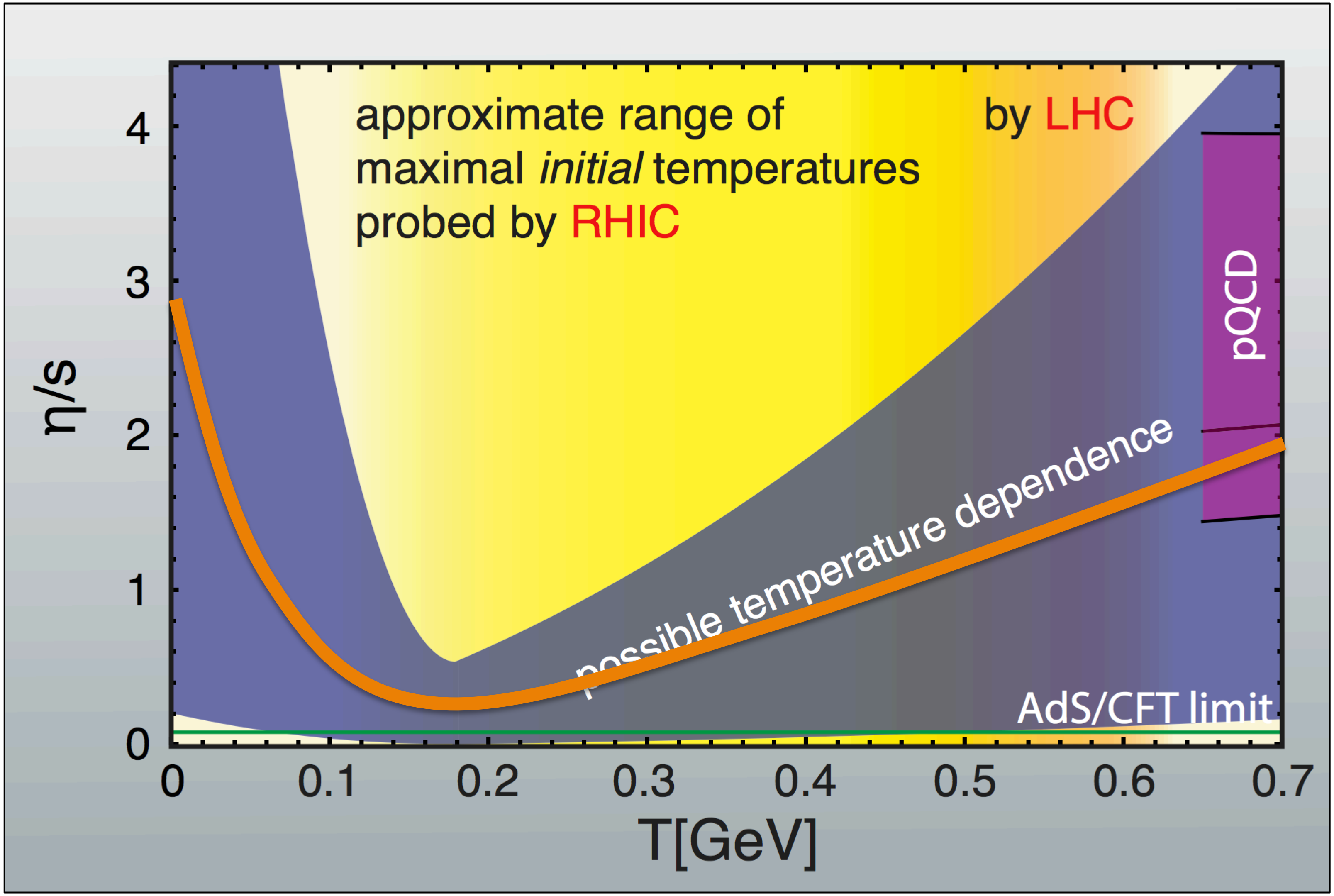

[Hot and Dense QCD Matter, Community Whitepaper 2014]

Anisotropic Hydrodynamics Basics

M. Martinez and MS, 1007.0889
W. Florkowski and R. Ryblewski, 1007.0130

Viscous Hydrodynamics Expansion

$$f(\tau,\mathbf{x},\mathbf{p}) = \underbrace{f_{\rm eq}(\mathbf{p},T(\tau,\mathbf{x}))}_{\text{Isotropic in momentum space}} + \delta f$$

Anisotropic Hydrodynamics Expansion

Treat this term "perturbatively"

[D. Bazow, U. Heinz, and MS, 1311.6720]

$$f(\tau,\mathbf{x},\mathbf{p}) = f_{\rm aniso}(\mathbf{p},\underbrace{\Lambda(\tau,\mathbf{x})}_{T_\perp},\underbrace{\xi(\tau,\mathbf{x})}_{\text{anisotropy}}\,) + \delta\tilde{f}$$

→ "Romatschke-Strickland" form in LRF

$$\boxed{f^{LRF}_{\rm aniso} = f_{\rm iso}\left(\frac{\sqrt{\mathbf{p}^2+\xi(\mathbf{x},\tau)p_z^2}}{\Lambda(\mathbf{x},\tau)}\right)}$$

$$\boxed{\xi = \frac{\langle p_T^2\rangle}{2\langle p_L^2\rangle} - 1}$$

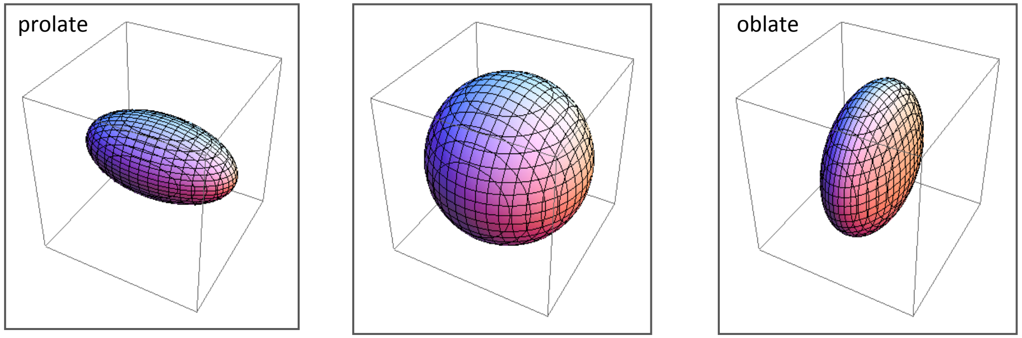

$-1 < \xi < 0$ $\qquad$ $\xi = 0$ $\qquad$ $\xi > 0$

Why spheroidal form at LO?

- What is special about this form at leading order?

$$f^{LRF}_{\rm aniso} = f_{\rm iso}\left(\frac{\sqrt{\mathbf{p}^2+\xi(\mathbf{x},\tau)p_z^2}}{\Lambda(\mathbf{x},\tau)}\right)$$

- Gives the ideal hydro limit when ξ=0 ($\Lambda \rightarrow T$)
- For longitudinal (0+1d) free streaming, the LRF distribution function is of spheroidal form; limit emerges naturally in aHydro

$$\xi_{\rm FS}(\tau) = (1+\xi_0)\left(\frac{\tau}{\tau_0}\right)^2 - 1$$

- Since $f_{iso} \geq 0$, the one-particle distribution function and pressures are ≥ 0 (not guaranteed in viscous hydro)
- Formalism reduces to 2nd-order viscous hydrodynamics in limit of small anisotropies

$$\frac{\Pi}{\mathcal{E}_{\rm eq}} = \frac{8}{45}\xi + \mathcal{O}(\xi^2)$$

Hints from Viscous Hydro

H. Song, PhD Dissertation, 0908.3656

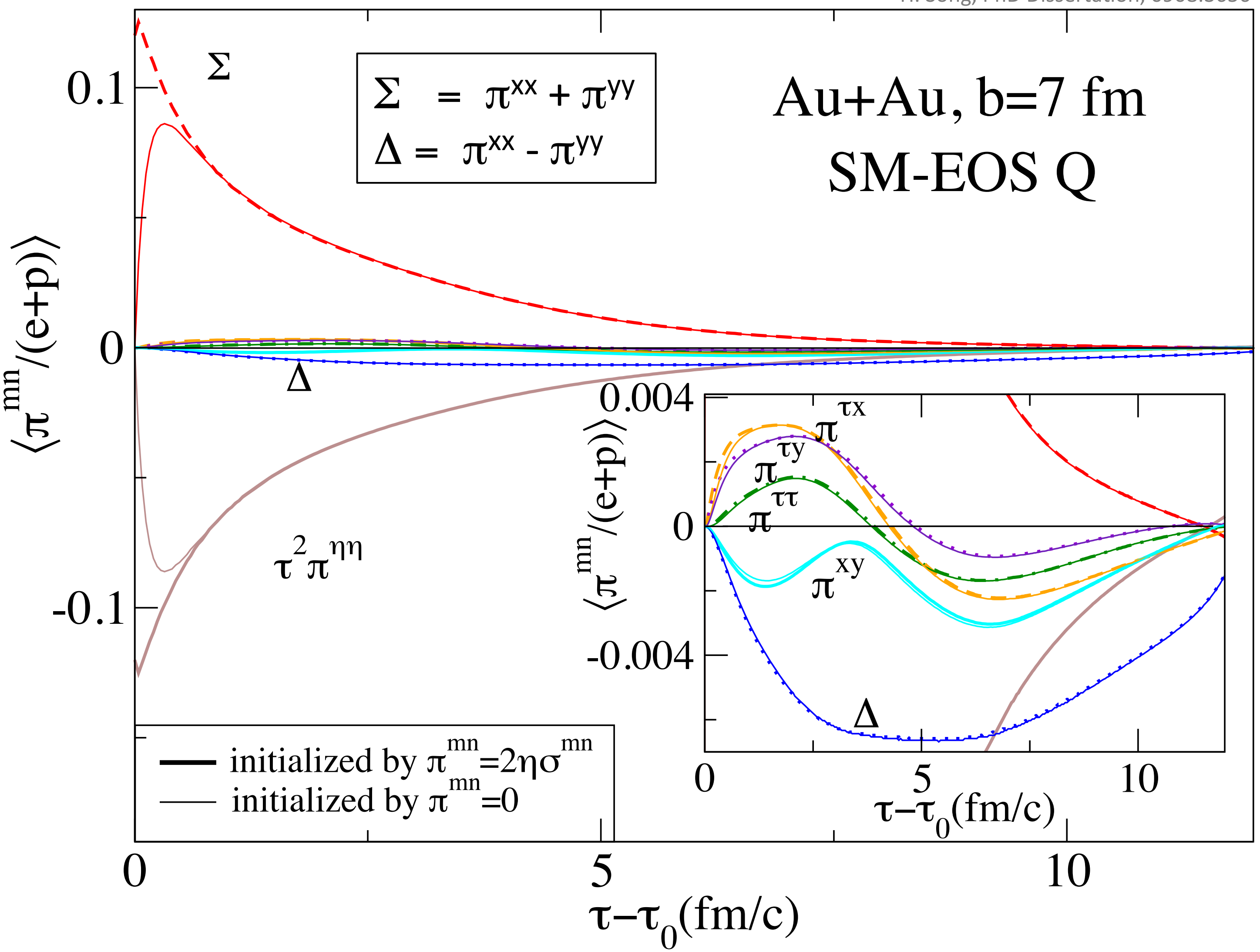

0+1d Pressure Anisotropy

$$\frac{1}{1+\xi}\partial_\tau\xi - \frac{2}{\tau} - 6\,\partial_\tau \log\Lambda = 2\Gamma\left[1-\mathcal{R}^{3/4}(\xi)\sqrt{1+\xi}\right]$$

$$\frac{\mathcal{R}'(\xi)}{\mathcal{R}(\xi)}\partial_\tau\xi + 4\,\partial_\tau \log\Lambda = \frac{1}{\tau}\left[\frac{1}{\xi(1+\xi)\mathcal{R}(\xi)} - \frac{1}{\xi} - 1\right]$$

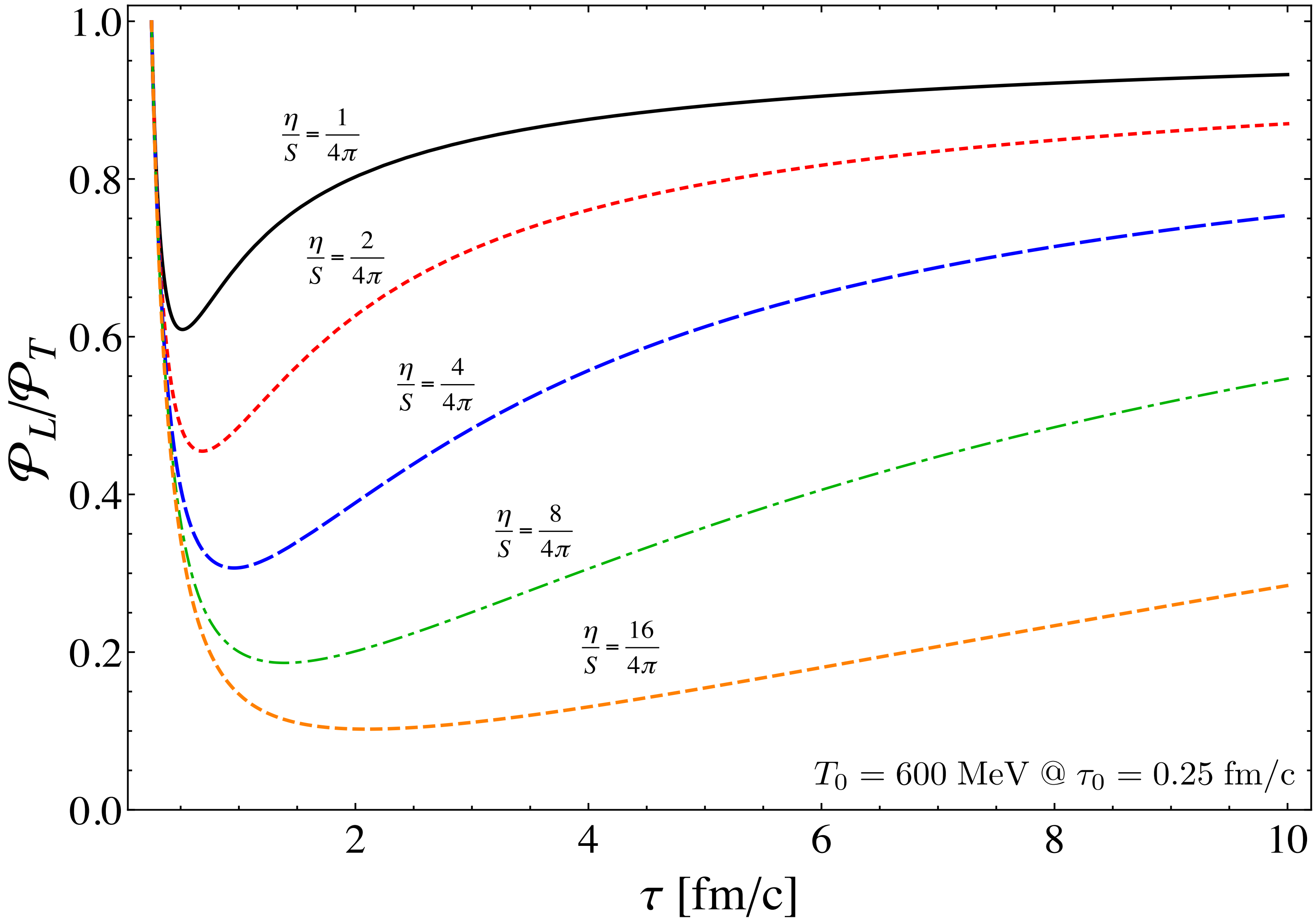

Including Transverse Dynamics

W. Florkowski and R. Ryblewski, 1103.1260
M. Martinez, R. Ryblewski, and MS, 1204.1473

- Allowing variables to depend on x and y, while still assuming boost-invariance, we obtain the "2+1d" dimensional aHydro equations
- Conformal system → four equations for four variables u_x, u_y, ξ, and Λ.

0th moment

$$\boxed{Dn + n\theta = J_0 \,.}$$

$$\boxed{\begin{aligned} D &\equiv u^\mu \partial_\mu \,, \\ \theta &\equiv \partial_\mu u^\mu \,, \end{aligned}}$$

$$\boxed{u_0 = \sqrt{1 + u_x^2 + u_y^2}}$$

1st moment

$$\boxed{\begin{aligned} D\mathcal{E} + (\mathcal{E} + \mathcal{P}_\perp)\theta + (\mathcal{P}_L - \mathcal{P}_\perp)\frac{u_0}{\tau} &= 0 \,, \\ (\mathcal{E} + \mathcal{P}_\perp)Du_x + \partial_x \mathcal{P}_\perp + u_x D\mathcal{P}_\perp + (\mathcal{P}_\perp - \mathcal{P}_L)\frac{u_0 u_x}{\tau} &= 0 \,, \\ (\mathcal{E} + \mathcal{P}_\perp)Du_y + \partial_y \mathcal{P}_\perp + u_y D\mathcal{P}_\perp + (\mathcal{P}_\perp - \mathcal{P}_L)\frac{u_0 u_y}{\tau} &= 0 \,. \end{aligned}}$$

NLO aHydro

Viscous Hydrodynamics Expansion

$$f(\tau,\mathbf{x},\mathbf{p}) = \underline{f_{\rm eq}(\mathbf{p},T(\tau,\mathbf{x}))} + \delta f$$

Isotropic in momentum space

Anisotropic Hydrodynamics Expansion

$$f(\tau,\mathbf{x},\mathbf{p}) = f_{\rm aniso}(\mathbf{p},\underbrace{\Lambda(\tau,\mathbf{x})}_{T_\perp},\underbrace{\xi(\tau,\mathbf{x})}_{\text{anisotropy}}) + \delta\tilde{f}$$

Now let's treat this term "perturbatively"

[D. Bazow, U. Heinz, and MS, 1311.6720]

→ "Romatschke-Strickland" form in LRF

$$\boxed{f^{LRF}_{\rm aniso} = f_{\rm iso}\left(\frac{\sqrt{\mathbf{p}^2+\xi(\mathbf{x},\tau)p_z^2}}{\Lambda(\mathbf{x},\tau)}\right)}$$

$$\boxed{\xi = \frac{\langle p_T^2\rangle}{2\langle p_L^2\rangle} - 1}$$

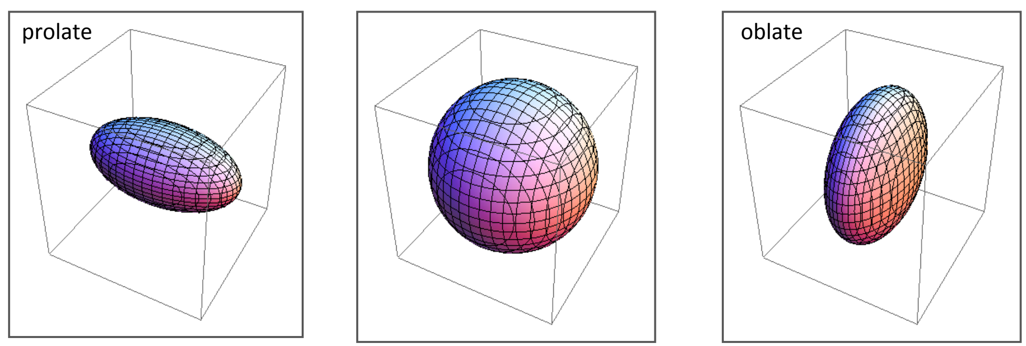

$-1 < \xi < 0$ $\qquad$ $\xi = 0$ $\qquad$ $\xi > 0$

Example: Entropy Generation

[D. Bazow, U. Heinz, and MS, 1311.6720]

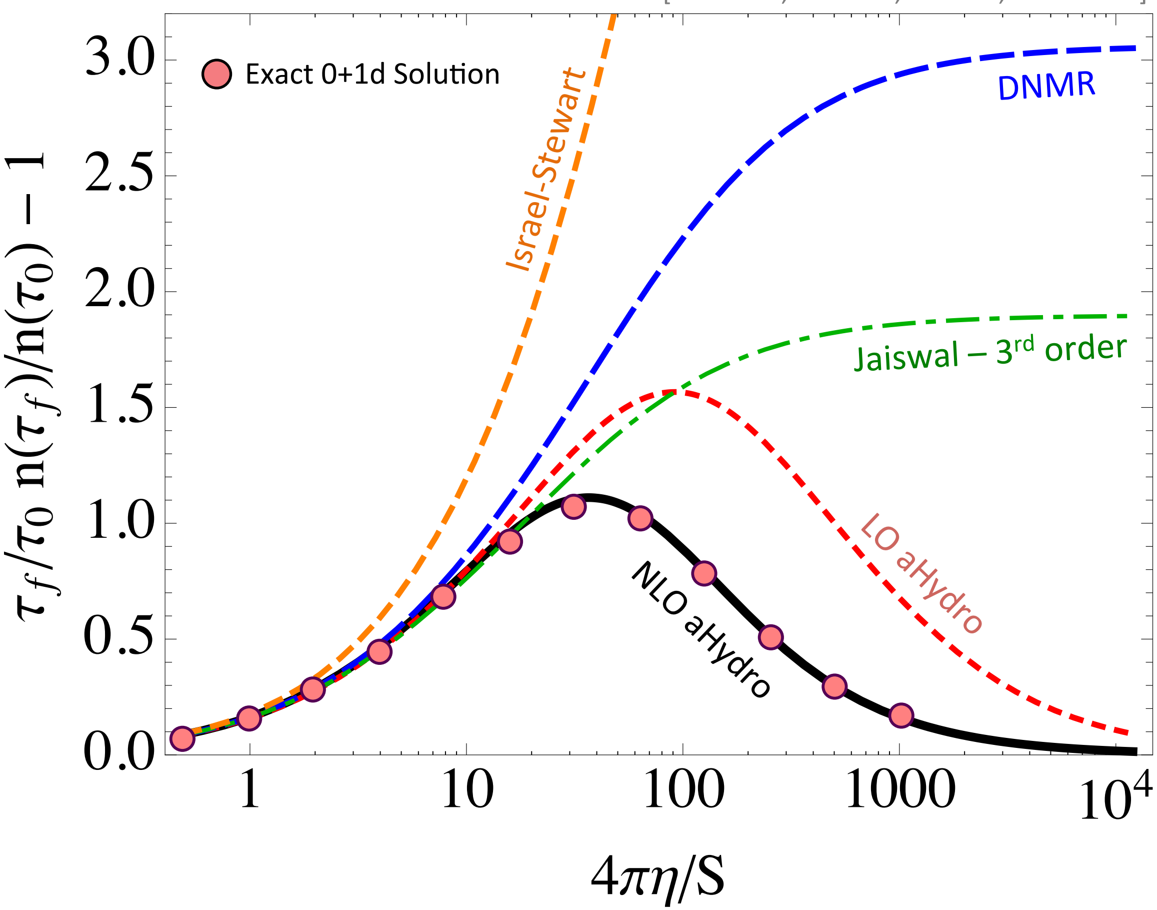

- Number (entropy) production vanishes in two limits: ideal hydrodynamic and free streaming limits
- In the conformal model which we are testing with, number density is proportional to entropy density

Spatiotemporal Evolution

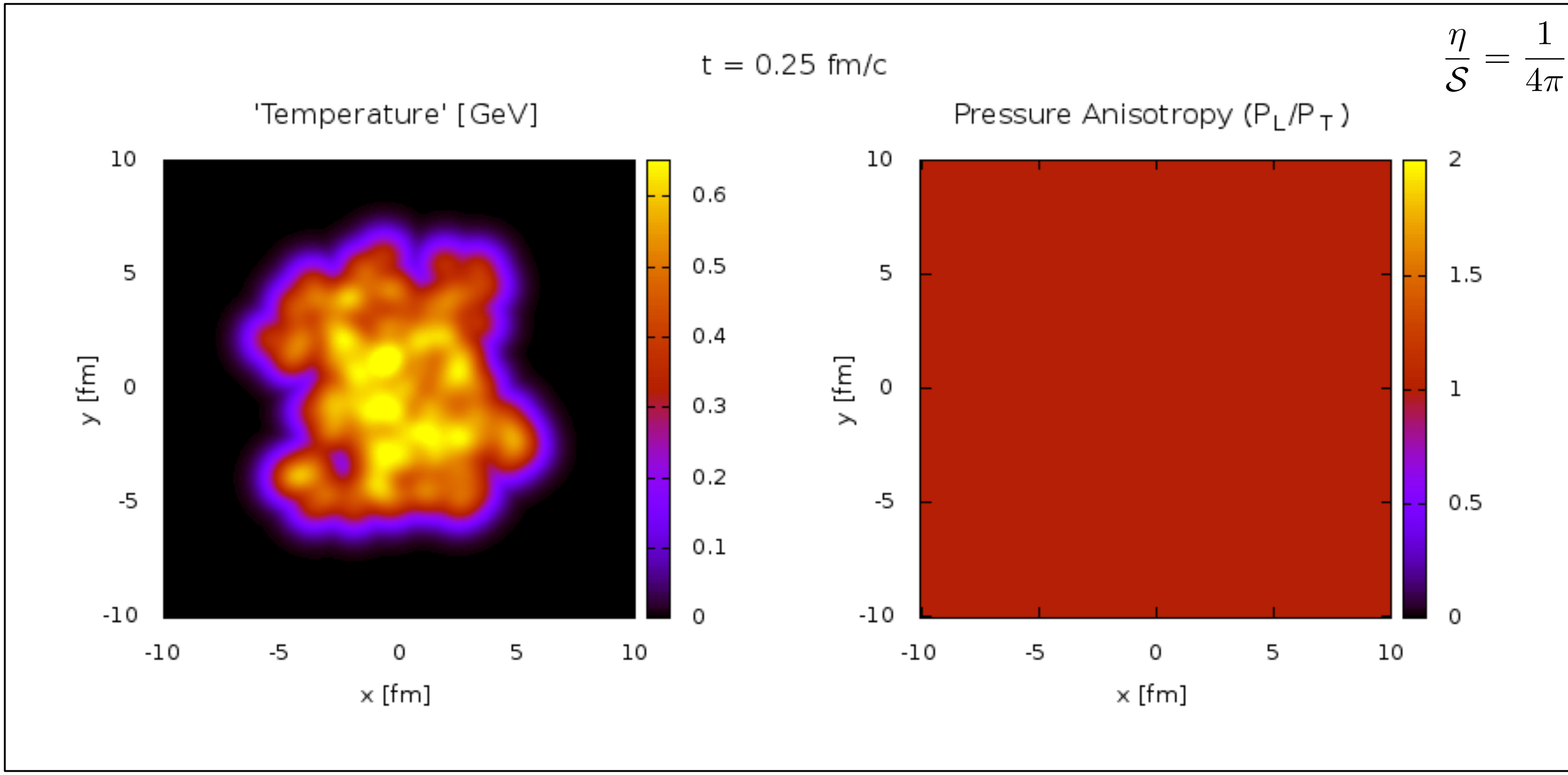

- Pb-Pb, b = 7 fm collision with Monte-Carlo Glauber initial conditions
  T_0 = 600 MeV @ τ_0 = 0.25 fm/c
- Left panel shows effective temperature; right shows pressure anisotropy

Anisotropic Heavy Quark Potential

Using real-time formalism one can express potential in terms of *static* advanced, retarded, and Feynman propagators

$$\boxed{V(\mathbf{r},\xi) = -g^2 C_F \int \frac{d^3\mathbf{p}}{(2\pi)^3}\,(e^{i\mathbf{p}\cdot\mathbf{r}}-1)\frac{1}{2}\left(D^{*L}_{R} + D^{*L}_{A} + D^{*L}_{F}\right)}$$

Real part can be written as

$$\mathrm{Re}[V(\mathbf{r},\xi)] = -g^2 C_F \int \frac{d^3\mathbf{p}}{(2\pi)^3}\, e^{i\mathbf{p}\cdot\mathbf{r}}\,\frac{\mathbf{p}^2+m_\alpha^2+m_\gamma^2}{(\mathbf{p}^2+m_\alpha^2+m_\gamma^2)(\mathbf{p}^2+m_\beta^2)-m_\delta^4}$$

With <u>direction-dependent masses</u>, e.g.

$$m_\alpha^2 = -\frac{m_D^2}{2p_\perp^2\sqrt{\xi}}\left(p_z^2\arctan\sqrt{\xi} - \frac{p_z\mathbf{p}^2}{\sqrt{\mathbf{p}^2+\xi p_\perp^2}}\arctan\frac{\sqrt{\xi}p_z}{\sqrt{\mathbf{p}^2+\xi p_\perp^2}}\right)$$

Anisotropic potential calculation: Dumitru, Guo, and MS, 0711.4722 and 0903.4703
Gluon propagator in an anisotropic plasma: Romatschke and MS, hep-ph/0304092

Full anisotropic potential

- Result can be parameterized as a Debye-screened potential with a direction-dependent Debye mass

$$V(r,\theta,\xi,p_{\rm hard}) = -C_F\alpha_s \frac{e^{-\mu(\theta,\xi,p_{\rm hard})r}}{r}$$

D Bazow and MS, 1112.2761; MS, 1106.2571.

- The potential also has an imaginary part coming from the Landau damping of the exchanged gluon!

$$V_{\rm R}(\mathbf{r}) = -\frac{\alpha}{r}\,(1+\mu\,r)\exp\left(-\mu\,r\right) + \frac{2\sigma}{\mu}\left[1-\exp\left(-\mu\,r\right)\right] - \sigma\,r\,\exp(-\mu\,r) - \frac{0.8\,\sigma}{m_Q^2\,r}$$

Dumitru, Guo, Mocsy, and MS, 0901.1998

- This imaginary part also exists in the isotropic case [Laine et al hep-ph/0611300]

- Used this as a model for the free energy (F) and also obtained internal energy (U) from this.

$$V_{\rm I}(\mathbf{r}) = -C_F\alpha_s p_{\rm hard}\Big[\phi(\hat r) - \xi\left(\psi_1(\hat r,\theta) + \psi_2(\hat r,\theta)\right)\Big]$$

Burnier, Laine, Vepsalainen, arXiv:0903.3467 (aniso)
Dumitru, Guo, and MS, 0711.4722 and 0903.4703

Solve the 3d Schrödinger EQ with complex-valued potential

Obtain real and imaginary parts of the binding energies for the $\Upsilon(1s)$, $\Upsilon(2s)$, $\Upsilon(3s)$, χ_{b1}, χ_{b2}

Results for the Υ(1s) binding energy

Margotta, MS, et al, 1101.4651

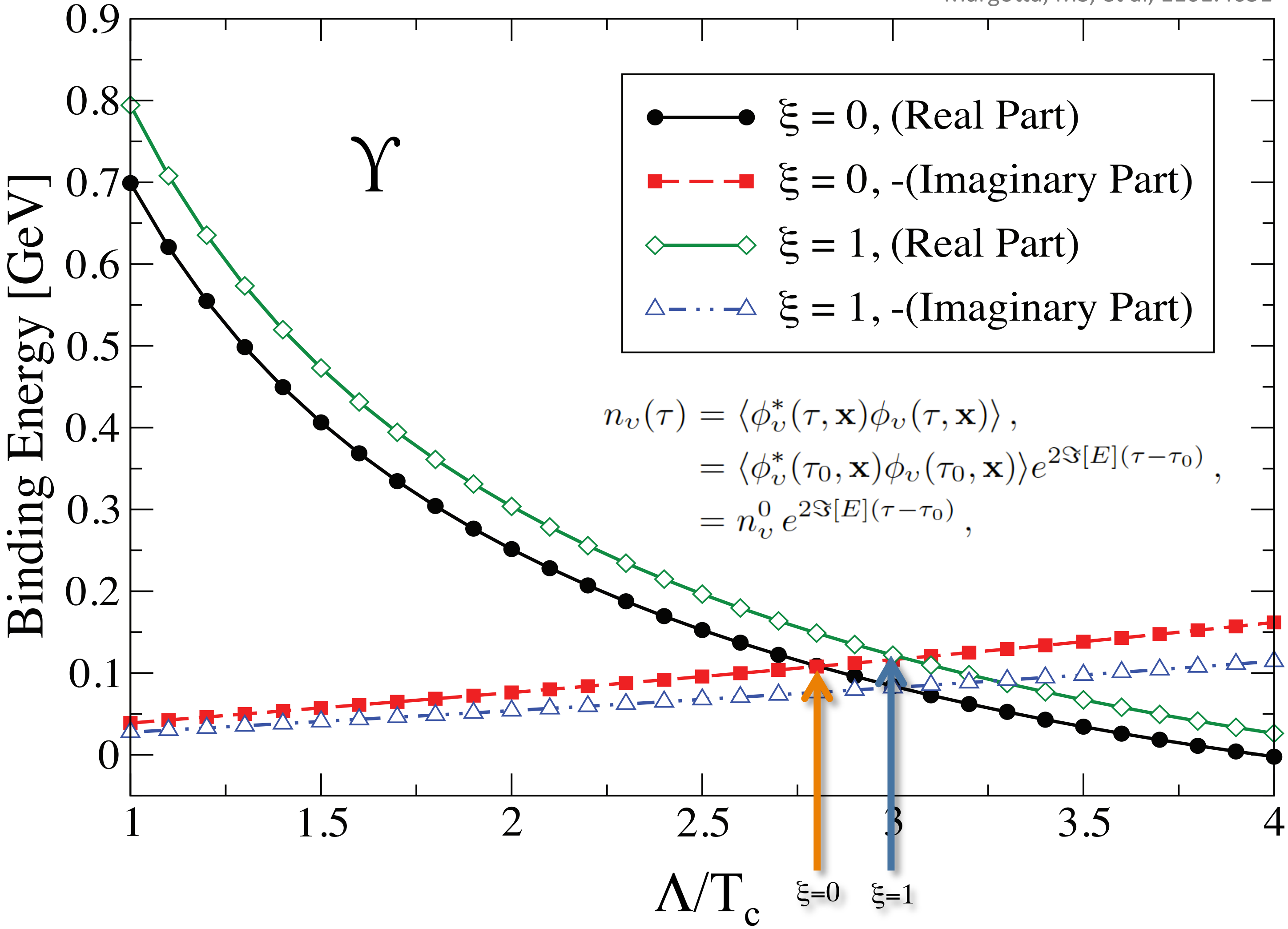

$$
\begin{aligned}
n_v(\tau) &= \langle \phi_v^*(\tau, \mathbf{x}) \phi_v(\tau, \mathbf{x}) \rangle \,, \\
&= \langle \phi_v^*(\tau_0, \mathbf{x}) \phi_v(\tau_0, \mathbf{x}) \rangle e^{2\Im[E](\tau-\tau_0)} \,, \\
&= n_v^0 \, e^{2\Im[E](\tau-\tau_0)} \,,
\end{aligned}
$$

Results for the χ_{b1} binding energy

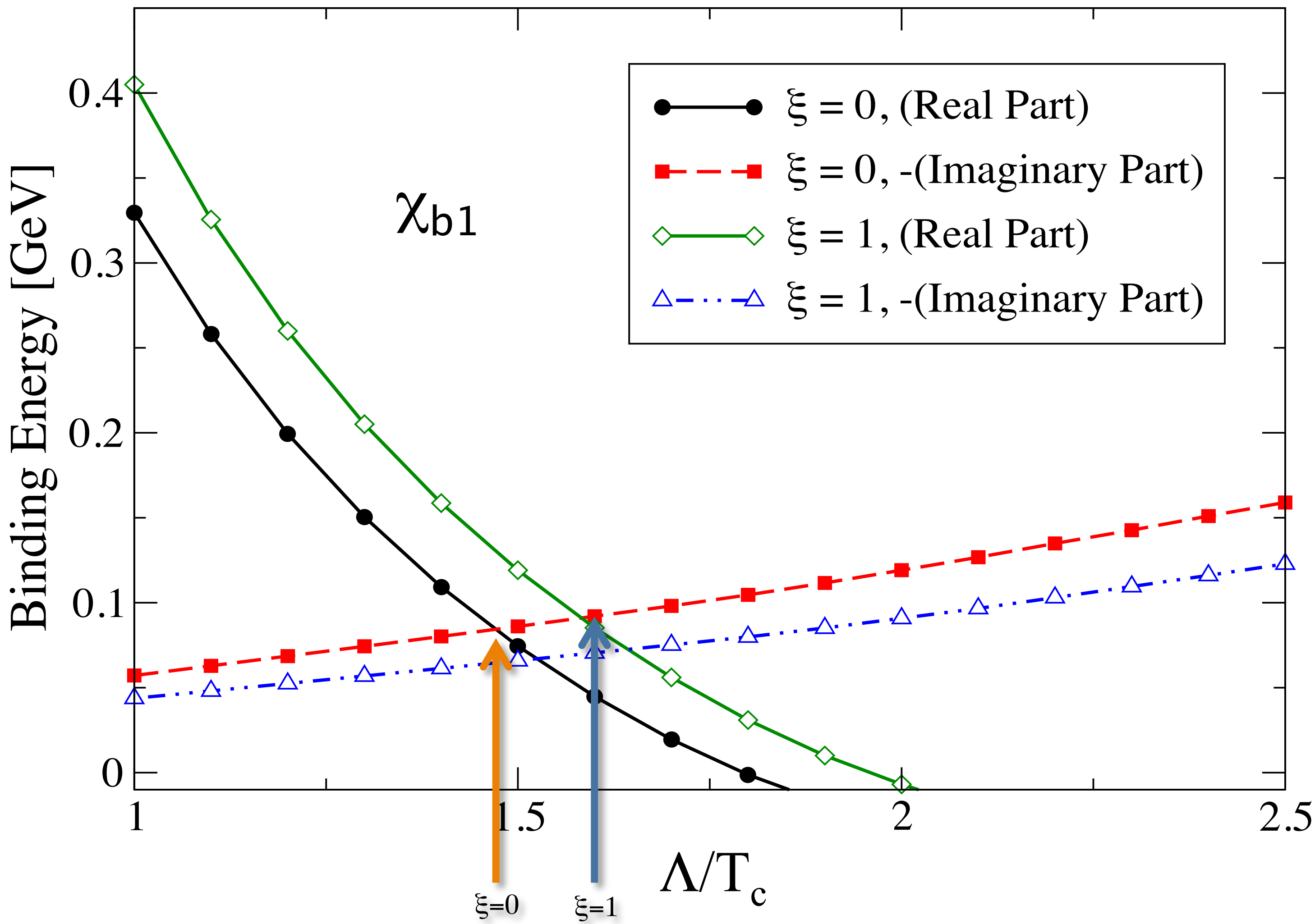

Spatiotemporal Evolution

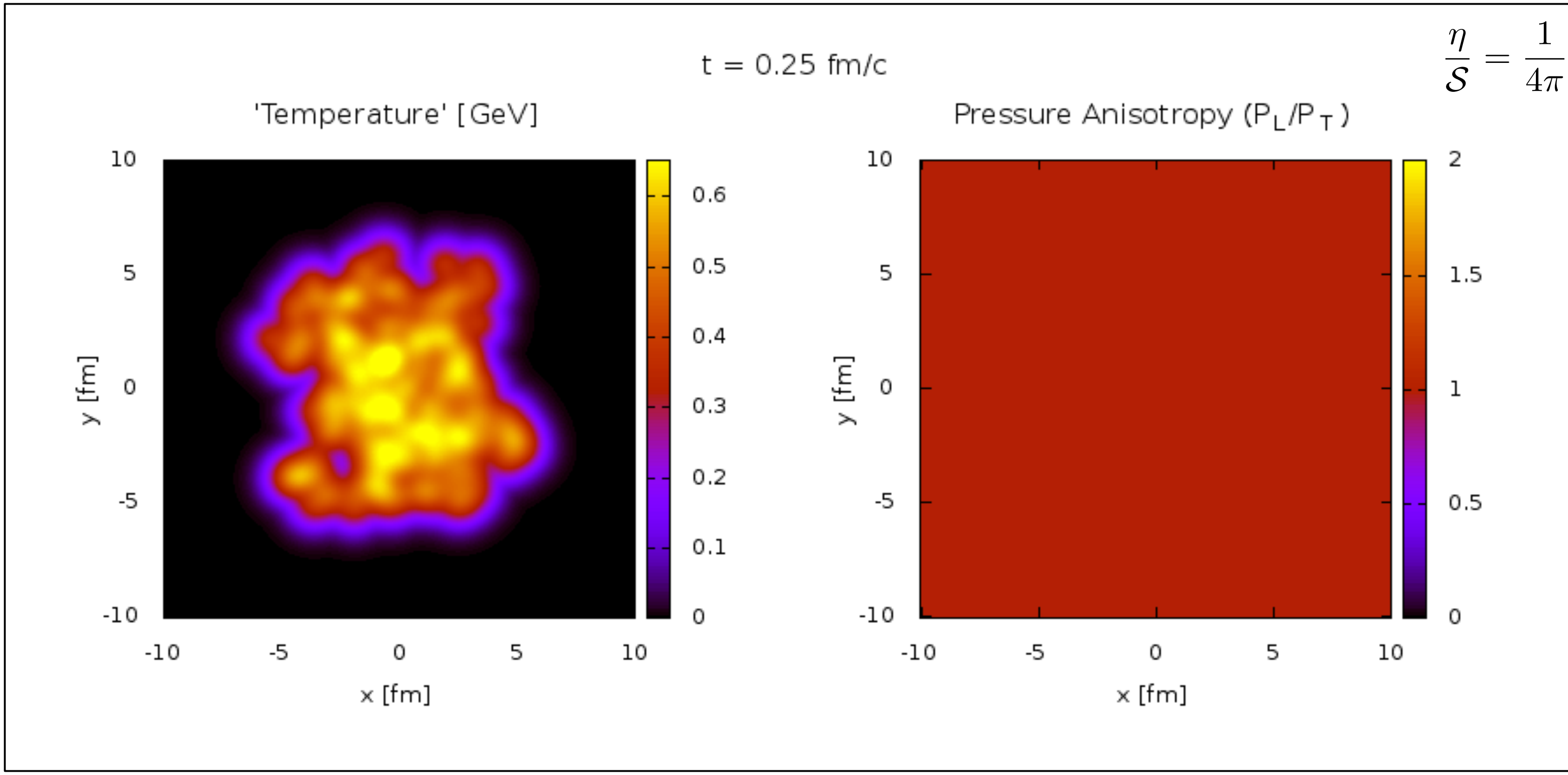

- Pb-Pb, b = 7 fm collision with Monte-Carlo Glauber initial conditions
  T_0 = 600 MeV @ τ_0 = 0.25 fm/c
- Left panel shows effective temperature; right shows pressure anisotropy

The suppression factor

- Resulting decay rate $\Gamma_T \equiv -2\,\mathrm{Im}[E_{bind}]$ is a function of τ, $x_\perp$, and ς (spatial rapidity). First we need to integrate over proper time

$$\bar{\gamma}(\mathbf{x}_\perp, p_T, \varsigma, b) \equiv \int_{\max(\tau_{\rm form}(p_T),\tau_0)}^{\tau_f} d\tau\, \Gamma_T(\tau, \mathbf{x}_\perp, \varsigma, b)$$

- From this we can extract R_{AA}

$$R_{AA}(\mathbf{x}_\perp, p_T, \varsigma, b) = \exp(-\bar{\gamma}(\mathbf{x}_\perp, p_T, \varsigma, b))$$

- Using the overlap density as the probability distribution function for quarkonium production vertices and geometrically averaging

$$\langle R_{AA}(p_T, \varsigma, b)\rangle \equiv \frac{\int_{\mathbf{x}_\perp} d\mathbf{x}_\perp\, T_{AA}(\mathbf{x}_\perp)\, R_{AA}(\mathbf{x}_\perp, p_T, \varsigma, b)}{\int_{\mathbf{x}_\perp} d\mathbf{x}_\perp\, T_{AA}(\mathbf{x}_\perp)}$$

State Suppression Factors, $R_{AA}{}^{i}$

D Bazow and MS, Nucl. Phys. A 879, 25 (2012); MS, PRL 107, 132301 (2011).

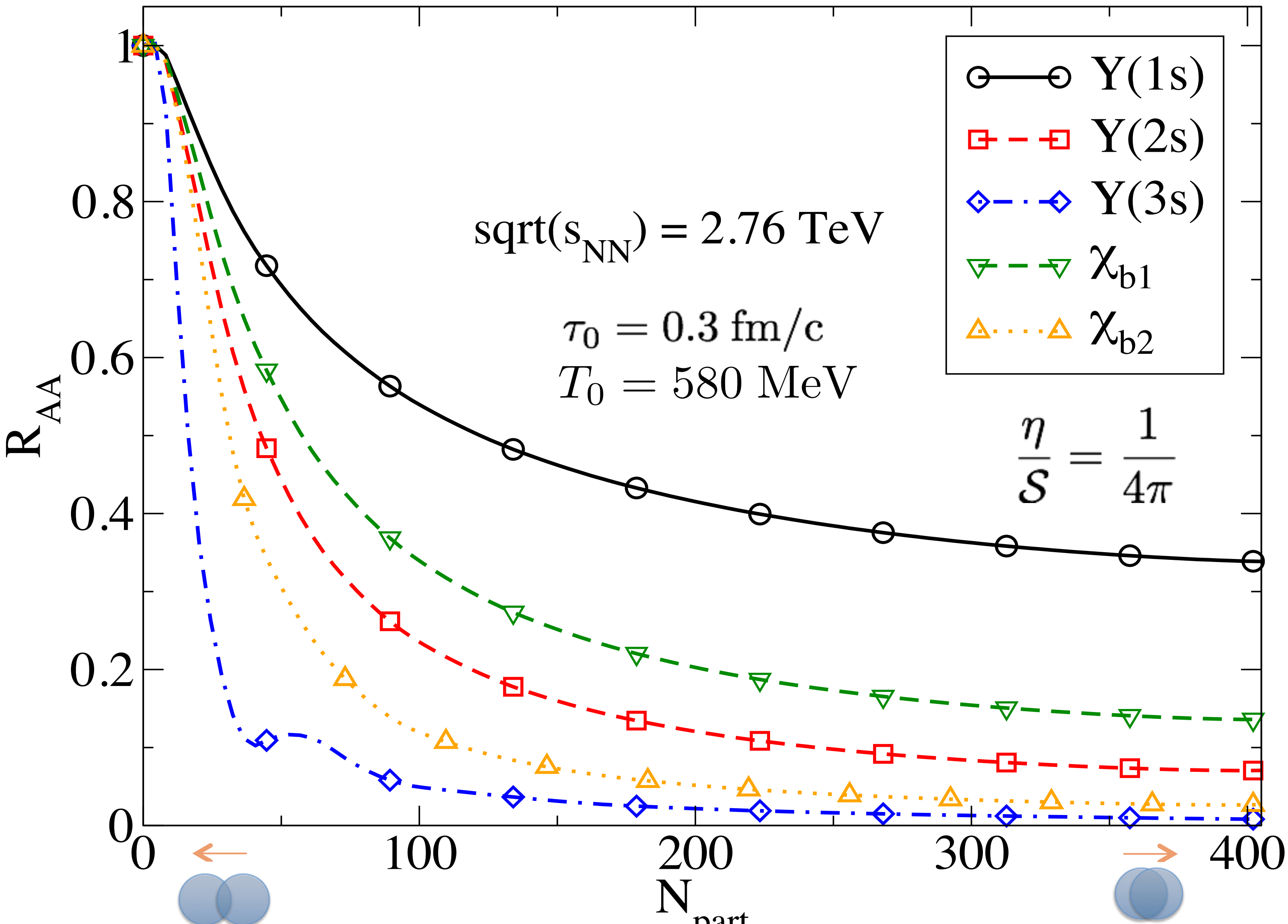

Inclusive Bottomonium Suppression

MS, arXiv:1207.5327; MS and D. Bazow, arXiv:1112.2761; MS arXiv:1106.2571

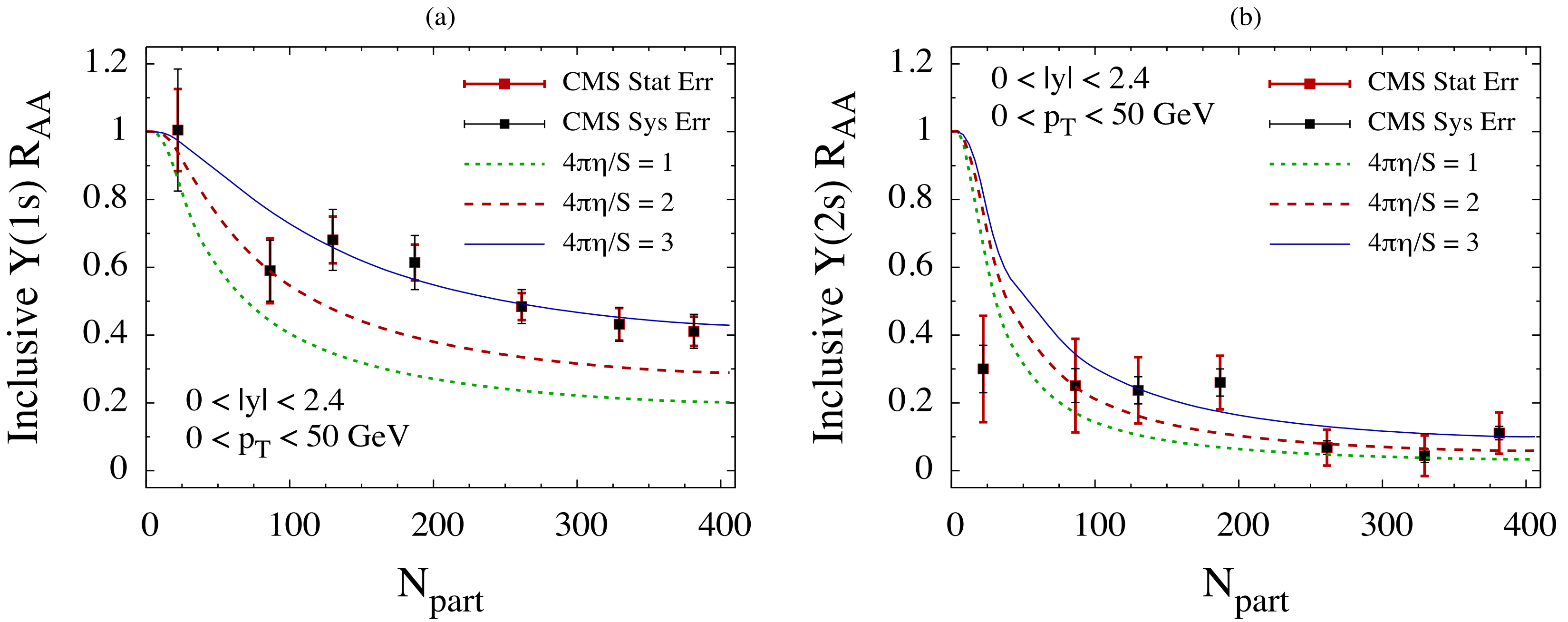

Computed inclusive ϒ(1s) and ϒ(2s) suppression including effects of feed-down, finite formation time, and aHydro evolution with anisotropic complex-valued quarkonium potential.

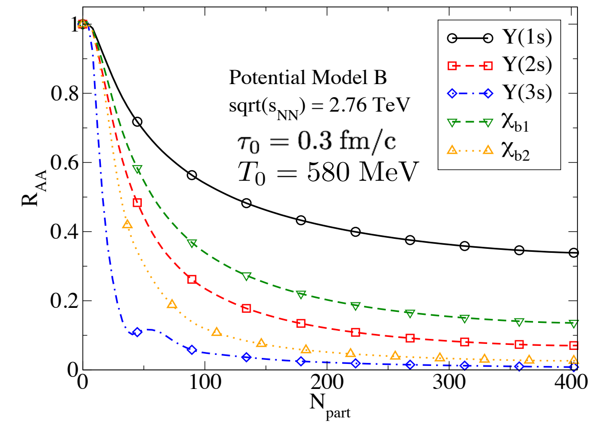

Conflict with ALICE data

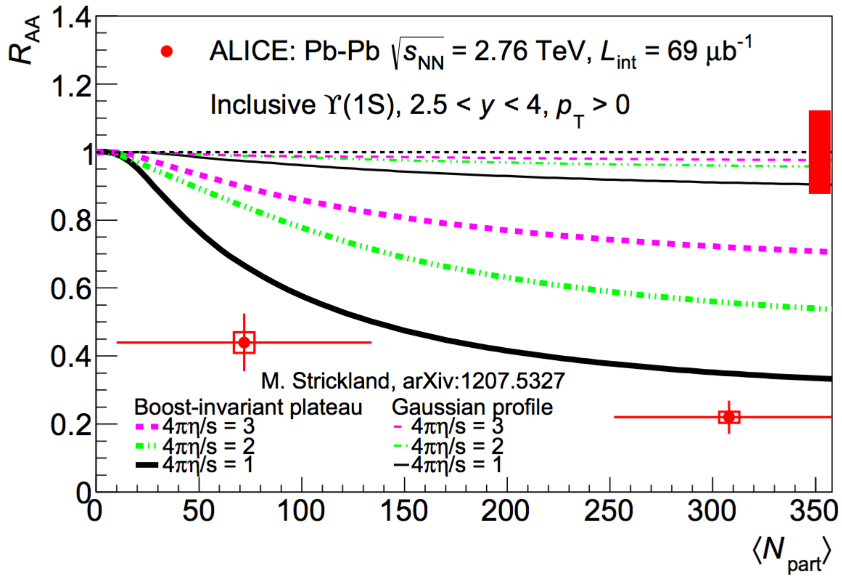

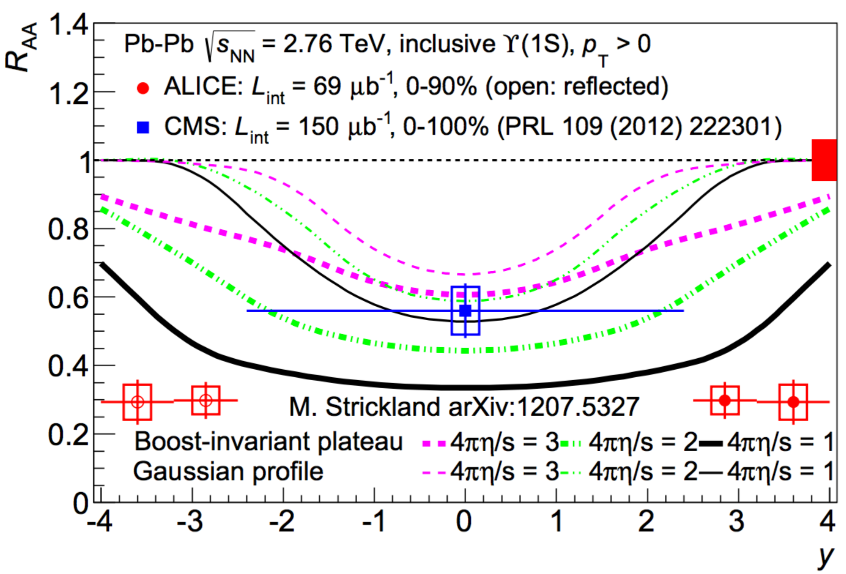

- Thermal suppression model has R_{AA} approaching 1 at forward/backward rapidity (T → 0)
- Using a Gaussian rapidity profile (Landau hydro) does not come close to the data
- Using a boost-invariant rapidity profile (Bjorken hydro) gives enhanced suppression, **but it also doesn't describe what was seen by ALICE!**
- IS effect?
- Assumption of small anisotropy breaking down?
- Poor/limited hydro modeling?
- Recombination?

(Some of) the problems with my calculation

- Small anisotropy expansion used for the imaginary part of the potential
- Dynamics was effectively 1+1d and used smooth initial conditions
- No regeneration
- No IS/CNM effects
- No singlet/octet transition Im[V]
- Simplistic model of how the anisotropy affects the long range part of the potential
- …

What am I working on now?

- We now have a 3+1d aHydro code that can handle fluctuating initial conditions ✔
- Using this code, we can have two fluids: the bulk can be ~ ideal hydro, while quarkonium states can be ~ free streaming; keep track of their full spatial distribution ✔
- We have generated our first 3d bottomonium RAA results ✔
- The main difference so far: rapidity-dependence of RAA gets slightly flatter but it still seems to be above the ALICE data ?
- Full anisotropy (ξ) dependence of the imaginary part of the potential (in progress)
- Include regeneration effects; density dependent local recombination
- Take initial R_{AA} from independent IS/CNM calculation; effects from IS/CNM and QGP suppression are multiplicative

Conclusions

- All signs point to an anisotropic QGP → need to self-consistently calculate rates including this effect
- At central rapidities, the model seems to work reasonably well
- For the 1s state, there is a large dependence on assumed value of η/s
- This offers the possibility to constrain η/s using bottomonium R_{AA}
- The strong suppression seen at forward rapidities is a challenge for the "thermal" model, but there is substantial room for improvement

- Backup slides -

1st Order Hydro – 0+1d

Additionally one finds for the first order distribution function

$$f(x,p) = f_{\rm eq}\left(\frac{p^\mu u_\mu}{T}\right)\left[1+\frac{p^\alpha p^\beta \pi_{\alpha\beta}}{2(\mathcal{E}+\mathcal{P})T^2}\right] \longrightarrow f_{\rm eq}\left(\frac{E}{T}\right)\left[1+\frac{\eta}{\mathcal{S}}\frac{p_x^2+p_y^2-2p_z^2}{3\tau T^3}\right]$$

- Distribution function becomes anisotropic in momentum space
- There are also regions where $f(x,p) < 0$
- Anisotropy and regions of negativity increase as τ or T decrease OR η/S increases

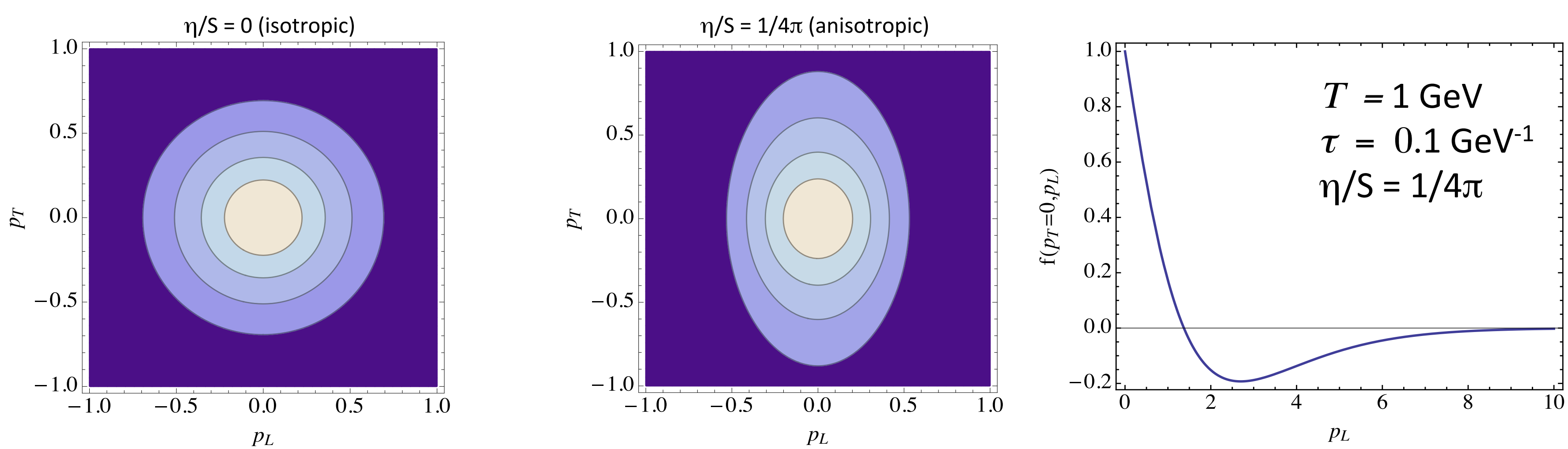

1st Order Hydro – 0+1d

Additionally one finds for the first order distribution function

$$f(x,p) = f_{\rm eq}\left(\frac{p^\mu u_\mu}{T}\right)\left[1+\frac{p^\alpha p^\beta \pi_{\alpha\beta}}{2(\mathcal{E}+\mathcal{P})T^2}\right] \longrightarrow f_{\rm eq}\left(\frac{E}{T}\right)\left[1+\frac{\eta}{\mathcal{S}}\frac{p_x^2+p_y^2-2p_z^2}{3\tau T^3}\right]$$

- Distribution function becomes anisotropic in momentum space
- There are also regions where $f(x,p) < 0$
- Anisotropy and regions of negativity increase as τ or T decrease OR η/S increases